Spatial Distribution of Cu Atoms Sputtered from Copper Target in RF Magnetron Sputtering

Toshio BANDAI

Department of Liberal Arts

Abstract

The spatial distribution of Cu atoms sputtered from a copper target in an RF magnetron sputtering was measured by the use of a quartz-crystal deposition monitor. At Argon pressure of 20 Pa, the angular distribution of sputtered atoms had a cosine-like distribution. At the lower Argon pressure, however, the deposition rate decreased at the front the target. This decrease was due to energetic neutral Ar atoms which bombarded and evaporated the growing films at the front of the target. The spatial distribution of Cu atoms sputtered from the target was simulated using the Monte Carlo method and compared with the observed result.

Key Words: sputter deposition, thin films, quartz-crystal deposition monitor, mean free path

1. Introduction

The magnetron sputtering[1] has found wide acceptance in the production of thin films. The primary use is the deposition of metals and insulators at low discharge pressures with high deposition rate and good film quality. The sputtering is a plasma-assisted process in the deposition of thin films.[2] The plasma is a glow discharge in which an anode is grounded and a negative voltage is applied to a cathode (target). The plasma shields the electric field through most of the chamber, and a cathode sheath of the order of 1 mm develops, and sustains most of the externally applied voltage.[1] A magnetic field is applied such that the arch-shaped magnetic field lines enter and leave through the target plate. Argon ions in the plasma, unconfined by the magnetic field, are accelerated toward the target and strike it at high energy. In addition to sputtering target material, the impact of the Argon ions produces secondary electron emission. The secondary electrons are accelerated back into the plasma along the magnetic field lines, and are confined near the target by the electric and magnetic filed. The electrons undergo a sufficient number of ionizing collisions to maintain the discharge. The discharge appears in the form of a brightly glowing ring where the magnetic field is tangent to the target.[3] Sputtering occurs in a corresponding track on the target. The discharge is non-uniform, and as a result, spatial non-uniformities occur in the deposition process.[4]

Growing films deposited by sputtering generally suffer a bombardment of energetic neutral atoms.[5] Its principal mechanism appears to be the reflection and neutralization of the energetic ions incident on the target surface. These energetic neutrals may have kinetic energies of up to several hundred eV,[5] and may induce significant damage in the properties of the deposited films. The magnitude of bombardment due to reflected neutrals would be reduced at high pressures due to scattering.

In this paper, in order to clarify the characteristics of sputtered atoms in the planar magnetron sputtering, the spatial distribution of Cu atoms sputtered from a copper

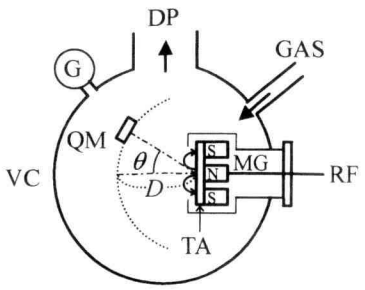

Fig. 1 A schematic view of an RF magnetron sputtering system equipped with a quartz-crystal deposition monitor. (DP) diffusion pump, (G) ion gauge, (GAS) inlet of Ar gas, (MG) magnetron sputter source, (QM) quartz-crystal deposition monitor, (RF) RF power input, (TA) target, (VC) vacuum chamber.

target is measured by the use of a quartz-crystal deposition monitor. The component reduced by the bombardment of energetic neutral atoms is estimated. The spatial distribution of Cu atoms sputtered from the copper target is simulated using the Monte Carlo method.

2. Experimental

Figure 1 shows a schematic view of the apparatus for monitoring the spatial distribution of sputtered copper atoms. This apparatus consisted of a sputtering chamber equipped with diffusion pump system, a magnetron source and a quartz deposition monitor. A copper metal target was 50 mm in diameter and 5 mm in thickness. The target was held to a magnetron source (LESKER MODEL TRS-002C). An RF power supply (KYOSAN MODEL RFK10) of 13.56 MHz was used.

Sputtering was done in a pure Ar atmosphere. The gas pressure in the sputtering chamber was varied from 0.5 Pa to 20 Pa. The Ar gas was introduced in the sputter chamber through a gas flow controller (MKS TYPE 246). The sputtering pressure was monitored by Schulz gauge and held constant using the gas flow controller.

The A quartz-crystal deposition monitor (INFICON MODEL XTM/2) was used for monitoring sputtered quantity. The change of the resonance frequency of the

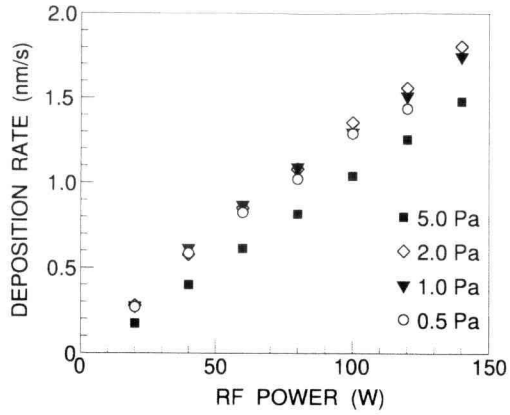

Fig. 2 Deposition rate of Cu film as a function of RF power for the case of Ar pressure at 5.0 Pa (■), 2.0 Pa(◇), 1.0 Pa (▼) and 0.5 Pa (○), respectively. The quartz-crystal monitor is positioned at $\theta = 0°$. The distance D from the target to the target to the monitor is fixed to 51 mm.

quartz-crystal was related to the quantity deposited on the monitor. The aperture of the quartz-crystal was 11 mm in diameter. The quartz-crystal monitor could be rotated around the target for measuring the angular distribution of sputtered Cu atoms. The angle θ of the quartz-crystal monitor to the normal of the target could be varied from −80° to +80°. Positive (negative) θ indicates the quartz-crystal monitor is positioned to the right (left) from the normal of the target. Also, the distance D from the target to the monitor could be varied from 51 to 100 mm. The data of the resonance frequency was acquired by a personal computer.

3. Experimental Results and Discussion

3.1 Deposition rate

Figure 2 shows the deposition rate as a function of RF power supplied to the Cu target for the case of Ar pressure at 5.0 Pa (■), 2.0 Pa(◇), 1.0 Pa (▼) and 0.5 Pa (○), respectively. The quartz-crystal deposition monitor is positioned at $\theta = 0°$. The distance D from the target to the quartz monitor is fixed to 51 mm. For the case of Ar pressure at 5.0 Pa, the deposition rate is proportional to the RF power. For the case of Ar pressure less than 2.0 Pa, however, the deposition rate deviates slightly from a linear relationship to the RF power.

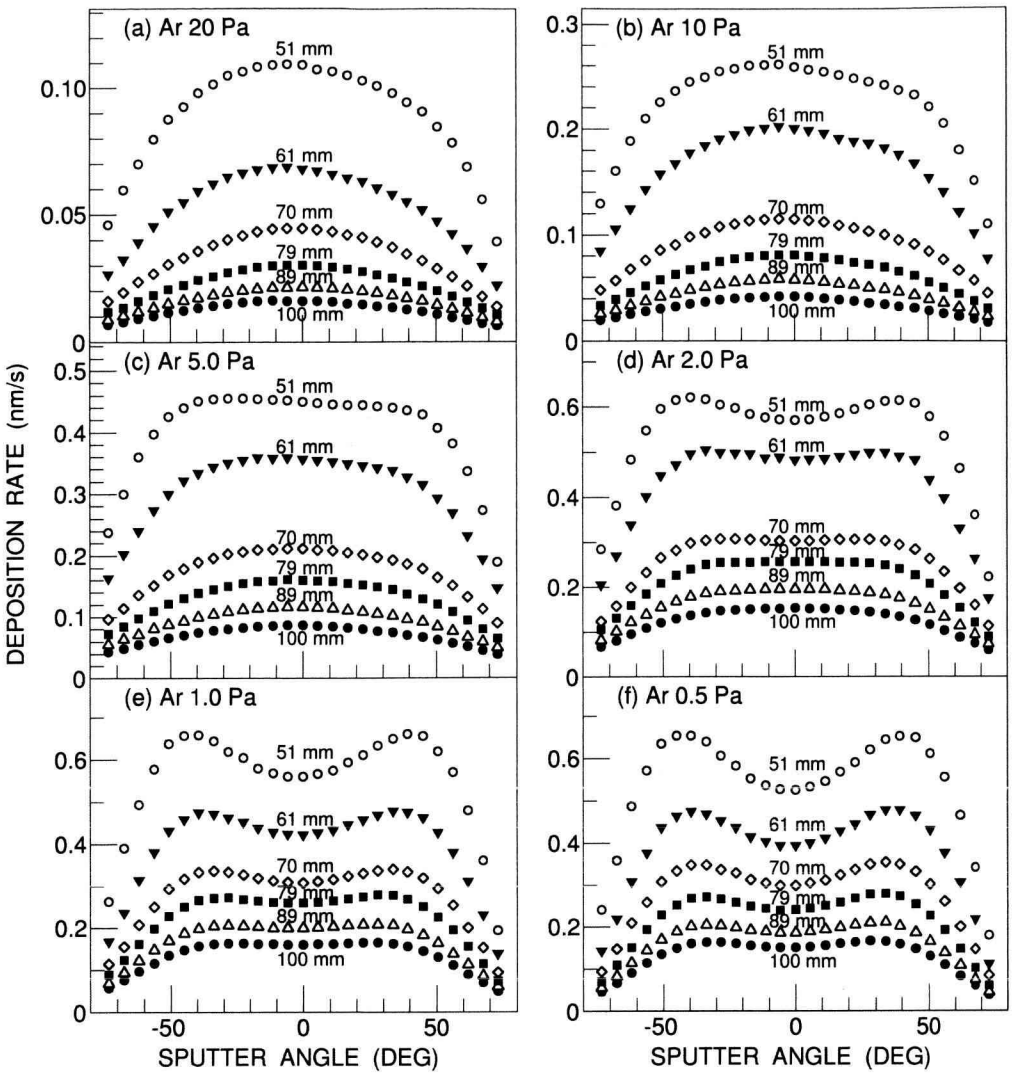

Fig. 3 Deposition rate of Cu film as a function of sputter angle θ for the case of Ar pressure at (a) 20 Pa, (b) 10 Pa, (c) 5.0 Pa, (d) 2.0 Pa, (e) 1.0 Pa and (f) 0.5 Pa. The distance from the target to the quartz-crystal monitor is 51 mm (○), 61 mm (▼), 70 mm (◇), 79 mm (■), 89 mm (△) and 100mm(●), respectively. The RF power supplied to the Cu target is fixed to 50 W.

Figure 3 shows the deposition rate of Cu film as a function of the sputter angle θ for the case of Ar pressure at (a) 20 Pa, (b) 10 Pa, (c) 5.0 Pa, (d) 2.0 Pa, (e) 1.0 Pa and (f) 0.5 Pa, respectively. The distance D from the target to the quartz-crystal monitor is 51 mm (○), 61 mm (▼), 70 mm (◇), 79 mm (■), 89 mm (△) and 100mm(●), respectively. The RF power supplied to the Cu target is fixed to 50 W. In Fig.3 (a) for the case of Ar pressure at 20 Pa, the deposition rate of sputtered Cu atoms has a cosine-like distribution. As the distance from the target to the quartz-crystal deposition monitor increases, the deposition rate decreases due to scattering by Ar atoms. The deposition rate is expected to be inversely proportional to the Ar pressure. As Ar pressure decreases from (b) 10 Pa to (a) 1.0 Pa, the deposition rate increases, but deviates from a cosine-like distribution. The deposition rate drops at $\theta = 0°$, and peaks at from $\theta = -30°$ to $\theta = -40°$ and at from $\theta = +30°$ to $\theta = +40°$. The decrease of deposition rate at $\theta = 0°$ is caused by the bombardment of energetic neutral Ar atoms.

To estimate the resputtered quantity by the

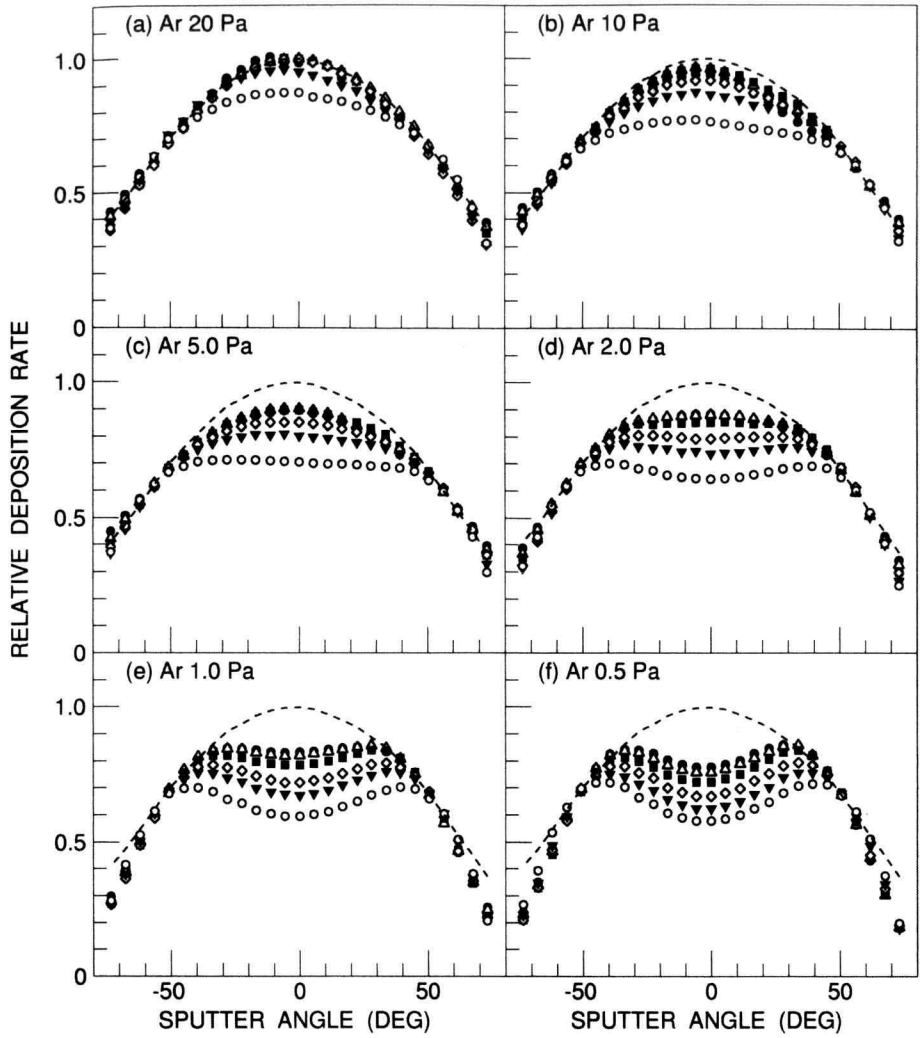

Fig. 4 Relative deposition rate as a function of sputter angle θ for the case of Ar pressure at (a) 20 Pa, (b) 10 Pa, (c) 5.0 Pa, (d) 2.0 Pa, (e) 1.0 Pa and (f) 0.5 Pa. The distance from the target to the quartz-crystal monitor is 51 mm (○), 61 mm (▼), 70 mm (◇), 79 mm (■), 89 mm (△) and 100mm(●), respectively. Dashed lines represent the deposition rate profile at Ar = 20 Pa and D = 100 mm. The RF power supplied to the Cu target is fixed to 50 W.

bombardment, we assign the deposition rate profile at Ar = 20 Pa and D = 100 mm to the profile without suffering from the bombardment. The effect of the bombardment in this state is expected to be the minimum in our measurement. Figure 4 shows the deposition ratio as a function of sputter angle θ for the case of Ar pressure at (a) 20 Pa, (b) 10 Pa, (c) 5.0 Pa, (d) 2.0 Pa, (e) 1.0 Pa and (f) 0.5 Pa, respectively. Dashed lines represent the deposition rate profile at Ar = 20 Pa and D = 100 mm. Observed profiles are fitted at $\theta = \pm 50°$ to that of Ar = 20 Pa and D = 100 mm. The differences between the dashed lines and the observed deposition rates are due to the resputtered quantity by the bombardment. The effect of the bombardment is in the range from $\theta = -40°$ to $+40°$. As the Ar pressure increases, the effect of the bombardment decreases due to scattering by argon atoms. As the distance from the target to the monitor increases, the effect of the bombardment also decreases due to scattering. Figure 5 shows the estimated deposition ratio at θ = 0° with addition of the quantity resputtered by the bombardment as a function of the distance from the target to the

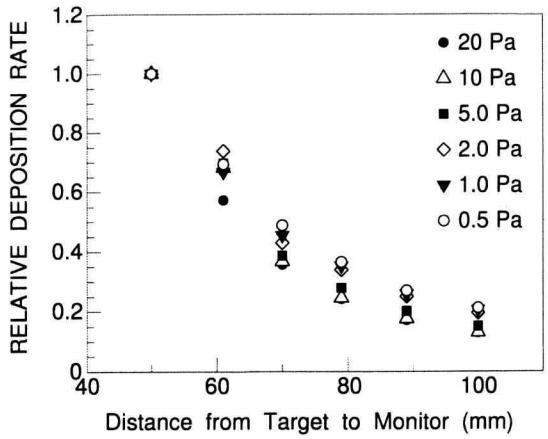

Fig. 5 The estimated deposition ratio at $\theta = 0°$ with addition of the quantity resputtered by the bombardment as a function of the distance from the target to the quartz-crystal monitor. Ar pressure is at 20 Pa (●), 10 Pa (△), 5.0 Pa (■), 2.0 Pa (◇), 1.0 Pa (▼) and 0.5 Pa (○), respectively. The RF power supplied to the Cu target is fixed to 50 W.

quartz-crystal monitor.

3.2 Simulation

We simulate the spatial distribution of copper atoms sputtered from the target using the Monte Carlo method.[6] Figure 6 shows a cross sectional view of a copper target, which has been sputtered for a long time. The depth of the groove is proportional to the quantity of copper atoms sputtered from the target. We assume that the probability $\rho(r)$ of Cu atoms sputtered from the position of radius r at the copper surface is,

$$\rho(r) = a \exp\left\{-b\,(r - r_0)^2\right\} + c \qquad (1)$$

By the least-square fitting to the groove in Fig.6, we obtain as a = 0.878, b = 0.00122 mm^{-2}, r_0 = 14.6 mm and c = 0.122. We assume that the probability of sputtered direction of Cu atom from the target is

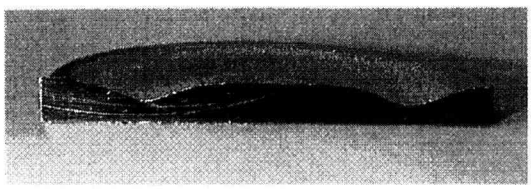

Fig. 6 A cross sectional view of a copper target, which has been sputtered for a long time.

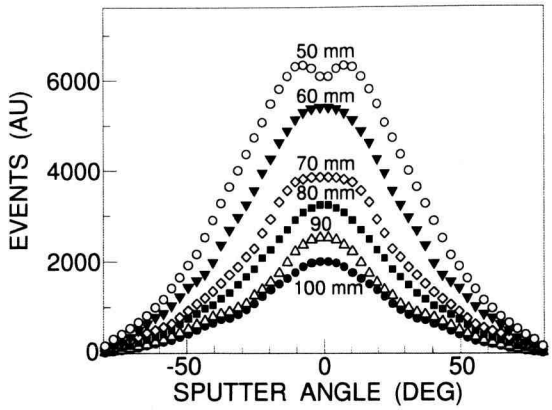

Fig. 7 Simulated result of sputtered atoms as a function of sputter angle θ for the case of the mean free path λ = 5 mm, and the distance D from the target to the quartz-crystal monitor is 50 mm (○), 60 mm (▼), 70 mm (◇), 80 mm (■), 90 mm (△) and 100 mm (●), respectively.

proportional to $\cos\phi$, where ϕ is an angle of sputtered direction to the normal of the target. As the sputtered Cu atom is neutral, the Cu atom moves linearly until collides with an Ar atom. The probability $\rho(d)$ of the Cu atom moving along the distance d without colliding with an Ar atom is,

$$\rho(d) = \exp\left(-\frac{d}{\lambda}\right) \qquad (2)$$

where λ is a mean free path.[7] It is also assumed that the moving direction of the Cu atom after colliding with an Ar atom is isotropic.

With these assumptions, we simulate the spatial distribution of sputtered copper atoms. A mean free path λ in the approximation of Maxwell's law of velocity distribution is given by,

$$\lambda = \frac{1}{\sqrt{2}\,\pi(\sigma_{Cu} + \sigma_{Ar})^2 n} \qquad (3)$$

where σ_{Cu}= 0.256 nm and σ_{Ar}= 0.36 nm are diameters of Cu and Ar atoms, n is number density of Ar atoms. The mean free path is 4.5 mm at Ar = 0.5 Pa, and 0.11 mm at Ar = 20 Pa, respectively. Figure 7 shows the simulation result of sputtered atoms as a function of sputter angle θ for the case of the mean free path λ = 5 mm. The distance D from the target to the quartz-crystal monitor is 50 mm (○), 60 mm (▼), 70 mm (◇), 80 mm (■), 90

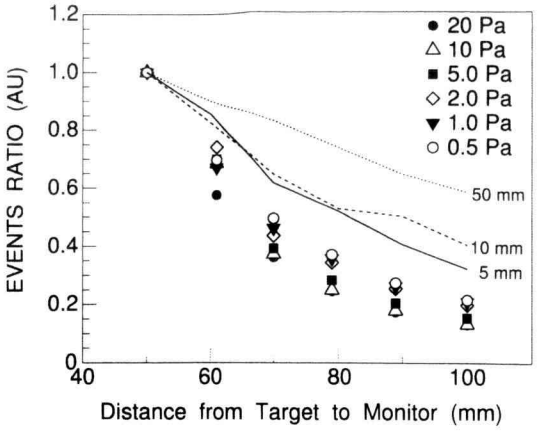

Fig. 8 Simulated ratio of sputtered atoms at $\theta = 0°$ as a function of the distance from the target to the quartz-crystal monitor for the case of mean free path λ = 50 mm (dotted line), 10 mm (dashed line) and 5 mm (solid line), respectively. For comparison, the observed deposition ratios already shown in Fig.5 are plotted.

mm (△) and 100 mm(●), respectively. The angular distribution of Cu atoms deviates from a cosine- like distribution. Figure 8 shows the simulated ratio of sputtered atoms at $\theta = 0°$ as a function of the distance from the target to the quartz-crystal monitor for the case of mean free path λ = 50 mm (dotted line), 10 mm (dashed line) and 5 mm (solid line), respectively.

For comparison, the observed deposition ratios shown in Fig.5 are also plotted. At Ar pressure of 0.5 Pa, the mean free path is 4.5 mm in the approximation of Maxwell's law of velocity distribution. The observed deposition ratios are well below the curve for the case of mean free path λ = 5 mm. We have simulated also for the case of mean free path λ = 2 mm, but obtained angular distribution has a profile dropped to nearly zero at $\theta = 0°$, contrary to the observed result. We now plan to check the assumption of the Monte Carlo method.

The angular distribution of Cu atoms sputtered from the surface of target in an RF magnetron sputtering has not a cosine-like distribution as shown in Fig.4 (f). In order to get the mean free path of the sputtered Cu atoms, the spatial distribution of the energetic neutral Ar atoms is also needed. We are now preparing to measure the spatial distribution of energetic neutral Ar Atoms by a quadrupole mass spectrometer.

Conclusions

The spatial distribution of Cu atoms sputtered from a copper target in an RF magnetron sputtering is measured by the use of a quartz-crystal deposition monitor. At Argon pressure of 20 Pa, the deposition rate has a cosine-like distribution. Although the deposition rate increases at the lower argon pressure, energetic neutral Ar atoms bombarded and evaporated growing films in the range from $\theta = -40°$ to $+40°$. The spatial distribution of Cu atoms sputtered from the target is simulated using the Monte Carlo method and compared with the observed result.

Acknowledgments

The author would like to thank Prof. F. Sisido for providing the sputtering facility and Prof. T. Hilano for many useful discussions on computer programming.

References

1) J. A. Thornton, J. Vac. Sci. Technol. **15**(1987)171.
2) H. R. Koenig and L. I. Maissel, IBM J. Res. Develop. **14**(1970)168.
3) A. E. Wendt, M. A. Lieberman and H. Meuth, J. Vac. Sci. Technol. **A6**(1988)1827.
4) A. E. Wendt and M. A. Lieberman, J. Vac. Sci. Technol. **A8**(1990)902.
5) S. M. Rossnagel, J. Vac. Sci. Technol. **A7**(1989)1025.
6) T. G. Lewis and B.J.Smith, *Computer Principles of Modeling and Simulation*, (Houghton Mifflin, Boston, 1979), p.86.
7) J. S. Logan, J. H. Keller and R. G. Simmons, J. Vac. Sci. Technol. **14**(1977)92.